Available online at www.sciencedirect.com

ScienceDirect

Energy Procedia 81 (2015) 866 – 873

Energy Procedia

69th Conference of the Italian Thermal Engineering Association, ATI 2014

EGR systems employment to reduce the fuel consumption of a downsized turbocharged engine at high-load operations

Bozza Fabio[a], De Bellis Vincenzo[a]*, Teodosio Luigi[a]

[a]*Industrial Engineering Department, Mechanic and Energetic Section, University of Naples "Federico II", Naples, Italy.*

Abstract

In this work, a promising technique, consisting in an introduction of the external low pressure cooled EGR system, is analyzed by means of a 1D numerical approach with reference to a downsized spark-ignition turbocharged engine. The effects of various EGR amounts are investigated in terms of fuel consumption at full load operations. The proposed results highlight that EGR allows for increasing the knock safety margin. Fuel economy improvements however depend on the overall engine recalibration, consisting in proper settings of the A/F ratio and spark advance, compatible with knock occurrence. The numerical recalibration also accounts for additional limitations on the turbocharger speed, boost level, and turbine inlet temperature. The maximum BSFC improvement by the proposed solution is 5.9%.

Peer-review under responsibility of the Scientific Committee of ATI 2014

Keywords: EGR; 1D engine modeling; fuel economy; knock.

Nomenclature

A/F	Air-to-Fuel Ratio
BSFC	Brake Specific Fuel Consumption
BMEP	Brake Mean Effective Pressure
EGR	Exhaust Gas Recirculation
ICE	Internal Combustion Engine
$\dot{m}_a$	Air mass flow rate

* Corresponding author. Tel.: +39-081-7683264; fax: +39-081-2394165.
E-mail address: vincenzo.debellis@unina.it

Peer-review under responsibility of the Scientific Committee of ATI 2014
doi:10.1016/j.egypro.2015.12.134

$\dot{m}_{EGR}$	EGR mass flow rate
MFB	Mass Fraction Burned
PID	Proportional Integral Derivative
PMEP	Pumping Mean Effective Pressure
SA	Spark Advance
SI	Spark Ignition
TDC	Top Dead Center
VVA	Variable Valve Actuation
VVT	Variable Valve Timing
TIT	Turbine Inlet Temperature
WG	Waste-Gate Valve

1. Introduction

Nowadays, Spark Ignition (SI) internal combustion engines (ICEs) show more and more complex systems aiming to reduce the fuel consumption and CO_2 emissions [1], while maintaining the prescribed power/torque performance. The downsizing philosophy, consisting in the reduction of the total displacement and in coupling the engine to a turbocharger [2], represents a successful solution for SI ICE that allows for a BSFC improvement at part load. Indeed, for an assigned torque, a downsized engine works at a higher BMEP level and, for this reason, operates in a more efficient zone of the engine map, thanks to a reduced intake throttling and lower pumping losses [1],[2]. A further decrease in in the pumping work can be achieved through the adoption of VVA/VVT systems [3]. In addition, a downsized engine involves a reduction in the friction losses [4],[5].

The main drawback of the downsized-turbocharging solution verifies at high load, where the boost level becomes very high and risks of knocking combustions occur. A common strategy to avoid the knock is to delay the combustion phasing, penalizing the thermodynamic efficiency [6]. In addition, the delayed combustion involves an increase in the turbine inlet temperature (TIT), that is usually compensated by an enrichment of the air to fuel (A/F) ratio, with further BSFC penalizations [7].

Different solutions have been proposed in the recent years to overcome the above issues [8]. A promising solution is the recirculation of a large amount of inert exhaust gas in the cylinders. This can be obtained by proper valve strategies, such as an extended exhaust/intake valves overlapping [9], or by an external EGR circuit [10]. The latter solution allows for a cooling of the exhaust gas, with direct advantages both for the knock occurrence and the turbine inlet temperature [10]-[12].

In this paper, a small port-fuel injected turbocharged VVA engine is analyzed by a 1D approach [13], [14]. The engine model, developed in the GT-Power environment, has been validated both at full and part load [15], [16]. It is here modified with respect to the base configuration to account for the introduction of a low pressure EGR circuit. The simulations are performed for different engine speeds at full load. The engine model is implemented so that the knock-limited spark advance is automatically selected, while respecting prescribed limitations on the TIT, the turbocharger speed, and the boost level. The latter needs to be controlled to ensure a proper operation of the fuel injectors. The effects of different EGR amounts and A/F ratios are finally compared for four operating points.

2. Combustion, turbulence and knock sub-models description and tuning

In order to account for the complex interaction among several devices, great care in the simulation must be paid in properly modeling the combustion and knock processes. Actually, different EGR levels increase the burning duration, reduce the in-cylinder temperature and affect the engine-turbocharger matching. All the above variations have a substantial effect on the rate of heat release. For this reason, the combustion process and the turbulence phenomenon are properly described by sub-models introduced in GT-Power through user routines. The combustion process is modeled by the “fractal combustion model” [17], [18] which is a phenomenological model sensing both the combustion system geometry and the operating parameters, including the residual gas content. Turbulence is

described by a 0D sub-model [19], [20]. The combustion process modeling is of course linked to the in-cylinder turbulence evolution to detect the effects of different control settings on the engine performance.

Following a hierarchical 1D-3D approach [19], [20], the turbulence and combustion model tuning constants are selected in order to fit the in-cylinder 3D-derived turbulent intensity and the in-cylinder pressure cycles at full load operations, respectively. A satisfactory agreement between the numerical and experimental results is obtained [20]. The model consistency, in terms of fuel consumption predictiveness, has been proved at part load, too [16].

With the aim of describing knock occurrence, turbulence and combustion models are coupled to a chemical kinetic solver (CHEMKIN), able to detect the presence of autoignition phenomena in the end-gas. A reduced kinetic mechanism for the oxidation of iso-octane and n-heptane mixtures is specified. It was developed by Tanaka and Keck [21], [22] and includes 5 elements, 32 species and 55 reactions. The mechanism handles both low and high temperature reactions and is particularly tuned [23] to reproduce the end-gas conditions in a SI ICE. The knock index used in the following analyses quantifies the heat release due to the end-gas autoignition [24]. The commercial gasoline used in the experimental tests is schematized in the simulations as a mixture of iso-octane and n-heptane (98% and 2% in volume, respectively). More details about the knock model assessment and validation are included in [24], [25].

3. Numerical campaign description

Following the same previously described modeling approach, an external EGR circuit is virtually mounted on the base engine. A low pressure EGR circuit (Fig. 1) is modeled by a circular pipe of a constant diameter that links the ducts upstream the compressor and downstream the turbine. Recycled gas flow rate and temperature are controlled by an EGR valve and a cooler device, respectively. An enhanced cooling system, requiring a water cooled heat exchanger, is specified, realizing a recycled gas temperature of 433 K.

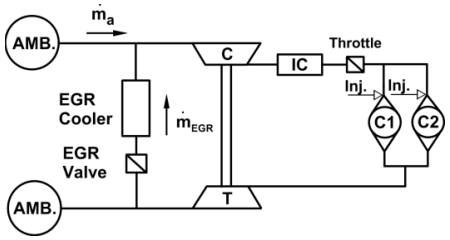

Fig. 1.Engine schematization

Four operating conditions are investigated (Table1) at full load. To respect knock limitations, a delayed combustion phasing is required in the base (no-EGR) calibration. In addition, the A/F ratio has to be enriched according to the engine speed mainly to maintain the TIT below a prescribed threshold level. A stated above, this also contributes to reduce knock risks.

Table1. Tested operating points

Case Number	Case label	Engine Speed, rpm	BMEP, bar	A/F Ratio,-	SA, deg BTDC
1	1500@15	1500	15.0	14.32	-12.3
2	2100@21	2100	20.8	12.88	-9.8
3	4000@20	4000	19.9	10.63	-1.8
4	5500@16	5500	16.1	10.75	5.9

For the examined cases, the model is firstly used to derive the knock index and the turbine inlet temperature in the base configuration. Then, different simulations are performed for each case with various A/F ratios and EGR valve openings. In this way, different EGR rates are obtained, here defined as:

$$EGR\ rate = \frac{\dot{m}_{EGR}}{\dot{m}_a + \dot{m}_{EGR}} 100 \quad (1)$$

The spark advance is searched in each case by a PID controller realizing the same knock intensity of the base configuration. The prescribed load level is finally matched acting on the waste-gate (WG) valve opening through a second controller.

4. Results discussion

The numerical results show that the adoption of an EGR system involves a BSFC reduction in most of the examined points. For the first considered operating point, i.e. 4000@20, an EGR increase always involves an improvement in the BSFC, (Fig. 2a), which also improves increasing the A/F ratio. The latter, however, also affects the combustion phasing (Fig. 2b) since a mixture leaning determines more critical knock conditions, mainly due to the reduced heat subtracted by fuel evaporation. Dashed lines in the above figures indicates operating conditions which do not respect limitations on the TIT, turbocharger speed and boost level. The optimal solution (denoted by a star) is obtained at an EGR rate of about 6%. A BSFC improvement of about 20 g/kWh with respect to the base calibration (square symbol), is attained at almost the same combustion phasing. Actually, the Fig. 3a shows that an EGR increase determines a higher boost level, due to the need to recover the prescribed load of 20 bar BMEP. A maximum boost of 2.6 bar hence determines a limitation on the maximum allowable EGR rate. Fig. 3b shows that the EGR induces a reduction on the TIT, while the A/F ratio has an opposite effect.

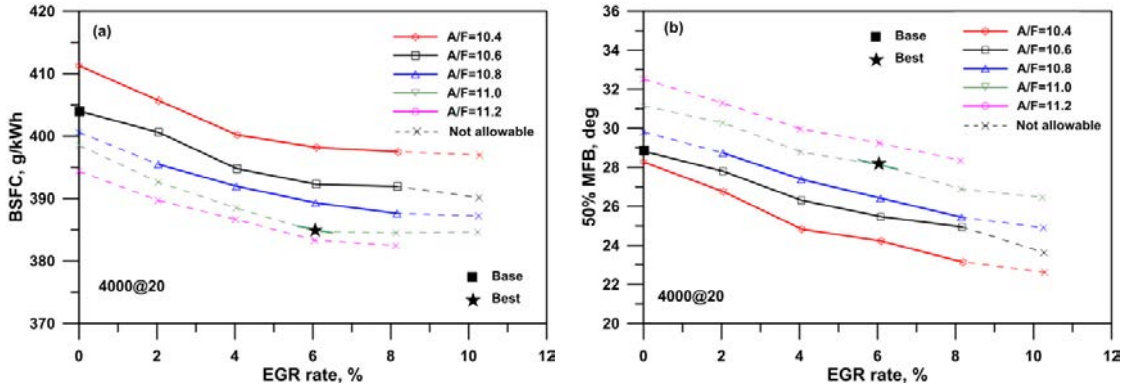

Fig. 2. BSFC (a) and 50% MFB (b) vs. EGR rate at 4000@20

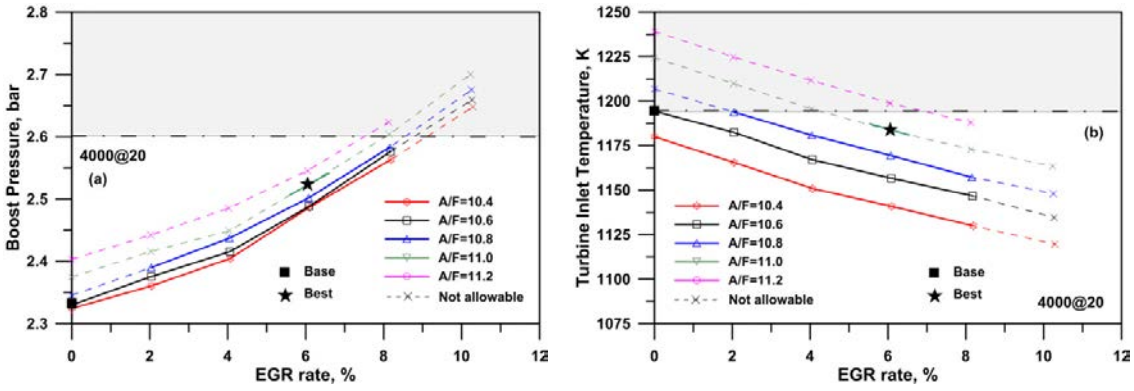

Fig. 3. Boost pressure (a) and TIT (b) vs. EGR rate at 4000@20

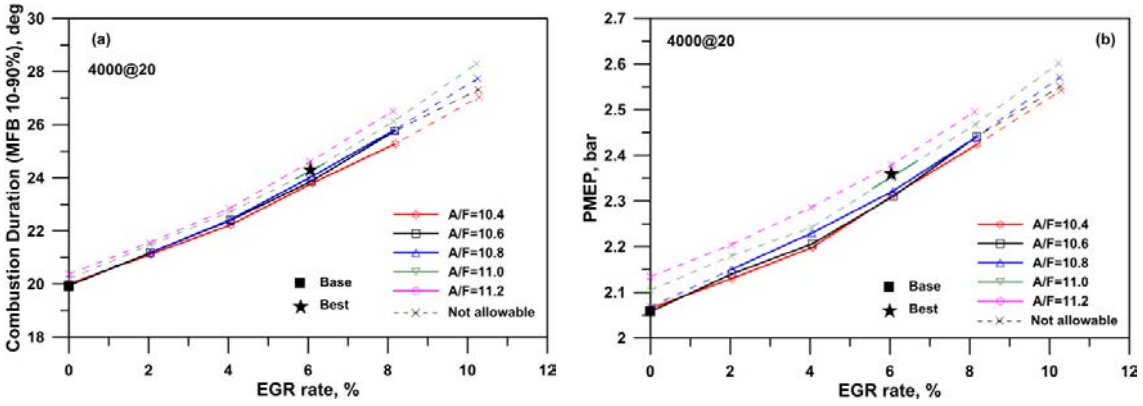

Fig. 4. Combustion duration (MFB 10-90%) (a) and PMEP (b) vs. EGR rate at 4000@20

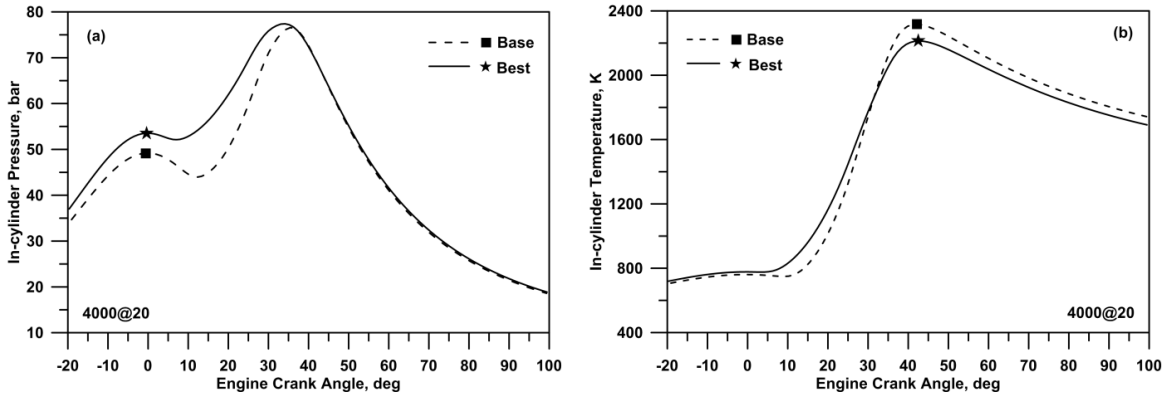

Fig. 5. In-cylinder pressure (a) and temperature (b) for the 'base' and 'best' calibrations at 4000@20

Fig. 4 highlights further effects caused by exhaust gas recycling on combustion duration and pumping losses (PMEP[†]). As expected, combustion duration substantially increases with EGR. Pumping losses rise as a function of EGR rate and A/F, as well. These effects are related to the increased backpressure induced by a higher WG closure, needed to reach the required power output. The above issues bound the BSFC advantages of the proposed solution, which however still remain significant.

The above considerations are confirmed by the analysis of the in-cylinder pressure and temperature cycles in the base and best calibration, reported in Fig. 5 In particular, the increased boost level required by the external-EGR determines a higher pressure at the TDC, while almost the same peak pressure is attained during combustion, mainly due to the slower burning rate. Indeed, the peak temperature is substantially reduced thanks to the increase in the heat capacity of the in-cylinder mixture caused by the higher inert content. Of course, this mechanism is the main reason of the improved knock resistance.

A very similar behaviour is also obtained in the maximum torque operating point, i.e. 2100@21, as shown in Fig. 6, resulting in a BSFC reduction of about 20 g/kWh. On the contrary, the operating condition characterized by the lowest speed and load, i.e. 1500@15, presents a peculiar response to the EGR increase. In fact, in this case, no benefits on BSFC can be obtained (Fig. 7a). Actually, at standard no-EGR operation, the best fuel consumption respecting all the imposed limitations is realized by a close to stoichiometric A/F ratio. An EGR increase at the

[†]The PMEP is conventionally assumed positive when the exhaust backpressure is higher than the boost pressure on the intake side

above constant A/F value now produces a relevant BSFC penalty, since the combustion phasing has to be delayed to avoid knocking combustions. This behavior appears consistent with the more critical knock operation usually verifying at low engine speeds. On the contrary, a decreasing BSFC vs EGR trend similar to the one reported in Fig. 2a can be only obtained at very rich air-fuel mixtures. At best, however, a BSFC level similar to the base no-EGR calibration can be attained.

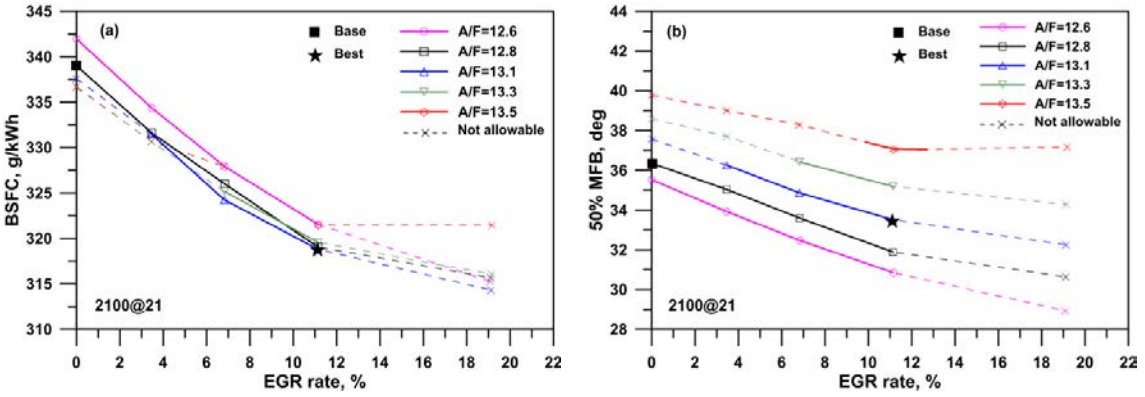

Fig. 6. BSFC (a) and 50% MFB (b) vs. EGR rate at 2100@21

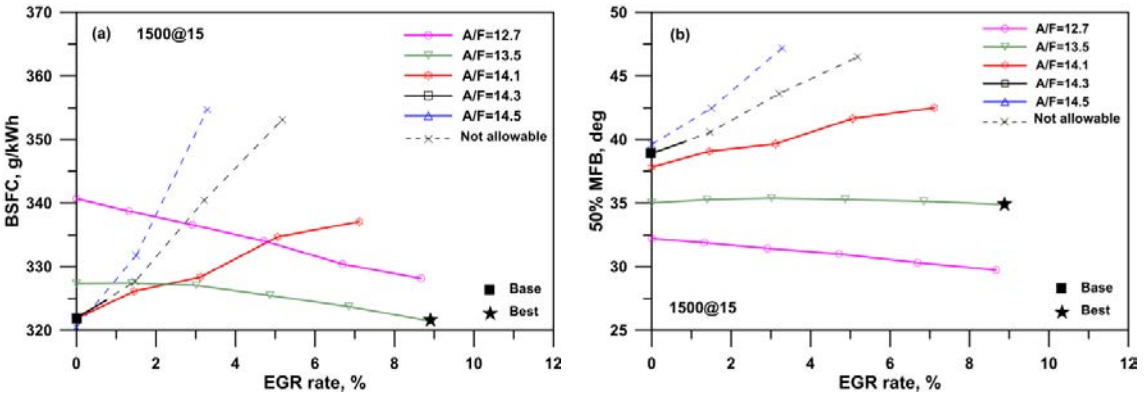

Fig. 7. BSFC (a) and 50% MFB (b) vs. EGR rate at 1500@15

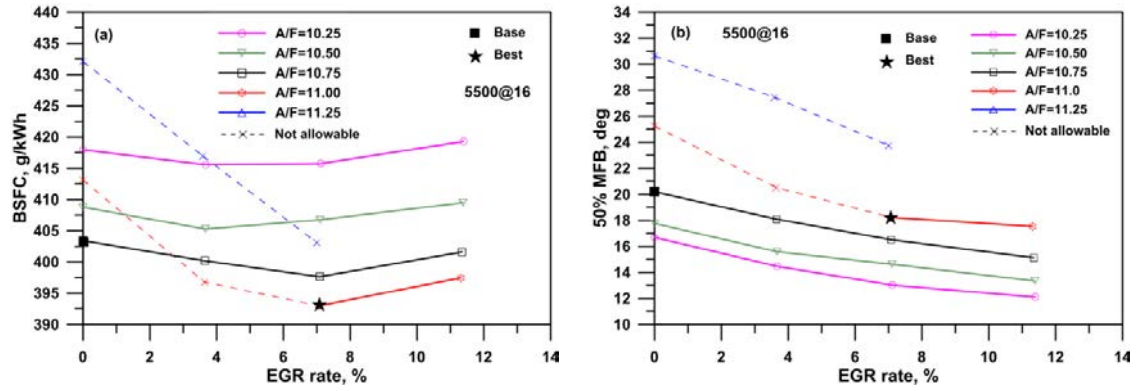

Fig. 8. BSFC (a) and 50% MFB (b) vs. EGR rate at 5500@16

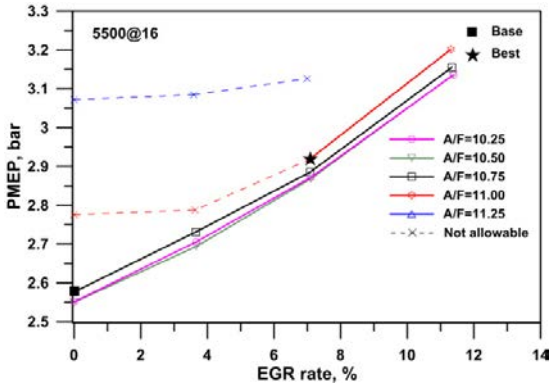

Fig. 9. PMEP vs. EGR rate at 5500@16

Finally, the maximum power output point is analyzed, i.e. 5500@16. Since high engine speed is now considered, results are much more controlled by the pumping loss changes induced by A/F ratio and EGR variations. Once again, however, the path to reduce the fuel consumption is a simultaneous slight A/F increase and a certain EGR level (Fig. 8a). Actual BSFC levels arise from a complex interaction among several effects including combustion phasing (Fig. 8b), pumping losses (Fig. 9) and respect of the assigned constrains.

Table2. Summary of the engine performance in the base and EGR-optimized calibrations

Base Calibration (EGR rate = 0 %)				Best EGR Calibration				
Case label	BSFC, g/kWh	50% MFB, deg	A/F, -	EGR rate, %	BSFC, g/kWh	ΔBSFC, %	50% MFB, deg	A/F, -
1500@15	321.9	38.9	14.3	8.9	321.5	-0.1	46.1	13.5
2100@21	339.0	36.4	12.9	11.1	318.8	-5.9	33.5	13.1
4000@20	404.0	28.8	10.6	6.1	384.7	-4.8	28.1	11.0
5500@16	403.4	20.2	10.75	7.1	393.0	-2.6	18.2	11.0

Table2 summarizes the trends previously shown in the different operating conditions. It can be noted that the maximum BSFC percent reduction (-5.9%) is obtained at 2100@21. Excepting the case at 1500@15, it is always observed that the EGR allows for a higher knock safety margin. This opportunity is exploited to realize a better phasing of the combustion and/or a leaning of the air/fuel mixture. Although a complex superimposition of various effects verifies, it is found that at low engine speeds the most limiting factor is the combustion timing, while pumping losses and mixture quality have a greater influence at high speeds. It is proved that EGR allows to mitigate the above issues, provided that a proper engine recalibration is applied.

Finally, it is the case to recall that, as well known, on the real engine, an increase in the residual gas involves a higher cyclic variation. The latter occurrence cannot be easily taken into account by the adopted 1D modeling approach. Nevertheless, the identified best solutions are characterized by a maximum EGR rate of 11%. Hence, a relevant penalization on the combustion stability during the actual engine operations is not to be expected, as experimentally shown in [26].

5. Conclusions

The paper reports numerical analyses showing the effects of the introduction of an external cooled EGR system on the fuel consumption of a small turbocharged twin-cylinder SI engine at full load operations. A 1D engine model is realized within GT-Power environment and it is properly tuned to reproduce the overall performance in the base configuration (no EGR).

Then, an external low pressure cooled EGR system is virtually mounted on the engine to promote an increase in EGR content. The numerical results show that, in the majority of the tested operating conditions, a significant BSFC

reduction is obtained. The above outcome is mainly ascribed to the decreased in-cylinder peak temperature induced by the higher amount of inert gas, that diminishes the knock risk and allows for an optimization of the combustion phasing and an air/fuel mixture leaning. However, secondary negative effects of the EGR strategy are a slower combustion rate and an increase in the pumping work. The best result is obtained at the operating point 2100@21, where a BSFC reduction of 5.9% is achieved with respect to the base configuration. At 1500@15, no fuel economy is detected, because of the penalizing effects of an excessive combustion delay, due to the higher knock risk. The proposed numerical methodology appears to be very helpful to identify the paths to improve the fuel economy at high load operations in presence of an external cooled EGR circuit.

References

[1] Fontana G, Galloni E. Variable valve timing for fuel economy improvement in a small spark-ignition engine. Applied Energy, 2009; 86:96–105.
[2] Wirth M, Schulte H. Downsizing and Stratified Operation – An Attractive Combination Based on a Spray-guided Combustion System, ICAT 2006, International Conference on Automotive Technologies Istanbul, November 17, 2006.
[3] Bozza F et al. A Theoretical Comparison of various VVA Systems for Performance and Emission Improvements of SI Engines. SAE Technical Paper 2001-01-0670, 2001, doi : 10.4271/2001-01-0670.
[4] Police G et al. Donwsizing of SI Engines by Turbo-Charging. Paper No ESDA2006-95215, pp 463-476, doi:10.1115/ESDA2006-95215.
[5] Amman H et al. The Effect of EGR on Low-Speed Pre-Ignition in Boosted SI Engines, SAE Technical Paper 2011-01-0339, 2011, doi: 10.4271/2011-01-0339.
[6] Shojaeefard M H et al. Cooled EGR for a Turbo Charged SI Engine to Reduce Knocking and Fuel Consumption, International Journal of Automotive Engineering, Vol. 3, Num. 3, September 2013.
[7] Grandin B, Ångström H. Replacing Fuel Enrichment in a Turbo Charged SI engine: Lean Burn or Cooled EGR, SAE Technical Paper 1999-01-3505, 1999, doi: 10.4271/1999-01-3505.
[8] Zhen X et al. The engine Knock analysis- An Overview, Applied Energy, April 2012, pages 628-636, doi : 10.1016/j.apenergy.2011.11.079.
[9] Jandquist H et al. Influence of valve overlap strategies on residual gas fraction and combustion in a spark-ignition engine at Idle, SAE Technical paper 972936, 1997, doi: 10.4271/972936.
[10] Fontana G, Galloni E. Experimental analysis of a spark-ignition engine using exhaust gas recycle at WOT operation; Applied Energy 87 (2010), 2187-2193.
[11] Galloni et al. Numerical analysis of EGR techniques in a turbocharged spark-ignition engine, Applied Thermal Engineering 39 (2012) 95-104.
[12] Kumano K, Yamaoka S. Analysis of Knocking Suppression Effect of Cooled EGR in Turbo-Charged Gasoline Engine, SAE Technical Paper 2014-01-1217, 2014, doi:10.4271/2014-01-1217.
[13] Fontana G et al. Experimental and numerical analyses for the characterization of the cyclic dispersion and knock occurrence in a small-size SI engine, SAE technical Paper 2010-32-0069, doi:10.4271/2010-32-0069.
[14] Fontanesi S et al. Analysis of Knock Tendency in a Small VVA Turbocharged Engine based on Integrated 1D-3D Simulations and Auto-Regressive Technique, SAE Int. J. Engines 7(1):72-86, 2014, doi:10.4271/2014-01-1065.
[15] De Bellis V et al. Fuel consumption optimization and noise reduction in a spark-ignition turbocharged VVA engine, SAE Int. J. of Engines 6(2):1262-1274, 2013, doi:10.4271/2013-01-1625.
[16] Bozza F et al. Strategies for Improving Fuel Consumption at Part-Load in a Downsized Turbocharged SI Engine: a Comparative Study; SAE Int. J. of Engines 7(1): 60-71, 2014, doi: 10.4271/2014-01-1064.
[17] Bozza F et al. Validation of a Fractal Combustion Model Through Flame Imaging. SAE Int. J. of Engines. 2006, Vol. 114-3, pp. 973-987. Journal Code E184774. ISSN 0096-736X. ISBN 0-7680-1689-4.
[18] Bozza F et al. Numerical and Experimental Investigation of Fuel Effects on Knock Occurrence and Combustion Noise in a 2-Stroke Engine, SAE Int. J. Fuels Lubr. 5(2):674-695, 2012, doi:10.4271/2012-01-0827.
[19] De Bellis V et al. Hierarchical 1D/3D Approach for the Development of a Turbulent Combustion Model applied to a VVA Turbocharged Engine. Part I: Turbulence Model. Energy Procedia. Volume 45, 2014, Pages 829–838.
[20] De Bellis V et al. Hierarchical 1D/3D Approach for the Development of a Turbulent Combustion Model applied to a VVA Turbocharged Engine. Part II: Combustion Model. Energy Procedia. Volume 45, 2014, Pages 1027–1036.
[21] Hu H, Keck J. Autoignition of Adiabatically Compressed Combustible Gas Mixtures, SAE 872110, 1987.
[22] Keck J, Hu H. Explosions of Adiabatically Compressed Gases in a Constant Volume Bomb, 21st International Symposium on Combustion, The Combustion Institute, pp. 521-529, 1986.
[23] Tanaka S et al. A Reduced Chemical Kinetic Model for HCCI Combustion of Primary Reference Fuels, Combustion & Flame, 132, pp. 219-239, 2003.
[24] Bozza F et al. A Knock Model for 1D Simulations Accounting for Cyclic Dispersion Phenomena, SAE Paper 2014-01-2554, 2014, doi: 10.4271/2014-01-2554.
[25] Siano D, Bozza F. Knock Detection in a Turbocharged S.I. Engine Based on ARMA Technique and Chemical Kinetics, SAE Technical Paper 2013-01-2510, 2013, doi:10.4271/2013-01-2510.
[26] Su J et al. Combined effects of cooled EGR and a higher geometric compression ratio on thermal efficiency improvement of a downsized boosted spark-ignition direct-injection engine, Energy Conversion and Management 78 (2014) 65-73.